THE SPRING RESEARCH ASSOCIATION

SOME OBSERVATIONS ON THE FATIGUE PROPERTIES IN BENDING AND THE FRACTURE BEHAVIOUR OF 0.28 mm PB102 PHOSPHOR-BRONZE STRIP

by

P. F. Timmins, M.Sc., A.Met., A.I.M., A.M.Inst.P.

Report No. 249

July 1975

THE SPRING RESEARCH ASSOCIATION

Report No. 249

SOME OBSERVATIONS ON THE FATIGUE PROPERTIES IN BENDING AND THE FRACTURE BEHAVIOUR OF 0.28 mm PB102 PHOSPHOR-BRONZE STRIP

SUMMARY

Fatigue and tensile tests have been carried out on specimens of BS 2870 PB102 extra-hard strip. S/N curves have been drawn for initial stresses of 75 and 225 N/mm^2. A modified Goodman diagram has been produced for this material with the upper boundary drawn at a stress level equivalent to the tensile 0.2% proof stress. Approximate reverse bending fatigue data obtained from the Goodman diagram have shown the behaviour of this material to be comparable to that reported by other investigators.

The failure behaviour in tension and fatigue have been examined fractographically and their mechanisms described. It has been suggested that the Fracture Mechanics approach be utilised to elucidate the nucleation, growth and fast propagation of fatigue failure.

CONTENTS

SOME OBSERVATIONS ON THE FATIGUE PROPERTIES IN BENDING AND THE FRACTURE BEHAVIOUR OF 0.28 mm PB102 PHOSPHOR-BRONZE STRIP

by

P. F. Timmins, M.Sc., A.Met., A.I.M., A.M.Inst.P.

1. INTRODUCTION

Phosphor-bronze (BS 2870 PB102) is one of the more common copper-based alloys used in spring applications for which high electrical conductivity is required. In strip form, the alloy is used in the manufacture of, for example, contacts and clips. Despite the fact that the alloy has been employed for many years in the industry, little information is available on the plane bending (one-side-of-zero) fatigue properties.[1] The present work was undertaken to provide these fatigue data and, at the same time, to examine the topography of crack propagation in the fatigue and tensile failure of PB102.

2. MATERIAL

The 5wt.% Sn-0.12wt% P-0.10wt.% Pb, balance Cu alloy used in this investigation was in the form of 17.5 mm wide by 0.28 mm thick strip, manufactured to meet BS PB102, in the extra-hard condition. Standard SRA strip specimens were used for tensile and fatigue testing.

3. EXPERIMENTAL PROCEDURE

3.1. Mechanical Testing

3.1.1. Tensile Testing

Discontinuous yielding (i.e. a yield drop) was not observed in the duplicate tests carried out on the specimens of PB102. The 0.1%, 0.2%, 0.5% proof stresses and U.T.S., together with percentage elongation-to-failure and Vickers hardness were measured.

3.1.2. Fatigue Testing

The specimens were positioned in a rig, designed for the testing of thin strip, by plane bending one-side-of-zero[2]. By means of load testing, the deflection necessary to apply the required stress was determined. These data were utilised to assemble the test strip and rig in one station of an eight-station, forced-motion, multiple-spring testing machine.

The strip specimens were tested at two levels of initial stress, namely 75 and 225 N/mm^2.

3.2. Metallography

Transverse and longitudinal specimens of the square-dressed edge strip were prepared for optical microscopy. In the unetched condition, fine particles, probably of Cu_2O, were observed. The etched microstructure was that of heavily deformed grains of duplex ($\alpha + \varepsilon$) solid solution.

4. EXPERIMENTAL RESULTS

4.1. Tensile Data

The calculated values of 0.1%, 0.2% and 0.5% proof stresses were 500, 620 and 650 N/mm^2, respectively. The calculated U.T.S. was 670 N/mm^2. A percentage elongation-to-failure of 2% was observed and the average Vickers hardness of the strips was 220. These data are given in Table I.

4.2. Fatigue Data

By varying the stress range applied to each specimen, the endurance was determined and accordingly maximum stress/cycles-to-failure (S/N) curves were constructed, as shown in Fig. 1. From these two curves, the maximum stresses at 10^7 cycles were found to be 375 and 475 N/mm^2 for initial stresses of 75 and 225 N/mm^2, respectively.

4.3. Fractography

Fractured tensile and fatigue specimens were examined by means of a scanning electron microscope (SEM), an instrument having a high resolution power such that one can look 'into' any fracture surface. With an SEM, an electron beam is used as a means of achieving illumination, rather than incident and reflected light, as used in conventional optical microscopes.

Typical tensile and fatigue fracture surfaces, observed by means of the SEM in the PB102 specimens, are shown in the fractographs in Figs. 2 and 3.

5. DISCUSSION

From the fatigue and tensile data, a modified Goodman diagram was constructed. This is shown in Fig. 4. The suggested maximum permissible operating stress is drawn at a level of stress equal to the tensile 0.2% proof stress, although for comparison purposes the U.T.S. line is also included. The difference between these two levels of stress is 50 N/mm^2. The use of the proof stress criterion is in itself becoming more acceptable, since recent work[3] has suggested that even in metals which exhibit discontinuous yielding, a true elastic limit may not be present because dislocation movement may occur at very low levels of applied stress. This type of plastic deformation is generally referred to as microplasticity.

Due to the lack of comparative bending fatigue data on PB102, an attempt was made to calculate the maximum stress in reversed plane bending from the data shown in Fig. 4 and to compare this with the previously published data[1].

The maximum stress in reversed plane bending, y, is related to the maximum stress for one-side-of-zero, f, by[2],

$$y = \frac{f}{2-R}$$

where R is the fatigue ratio $= \frac{f}{UTS}$.

If the formula is applied to the data shown in Fig. 4 using the following values:

$f = 340\ N/mm^2$

$U.T.S. = 670\ N/mm^2$

then $R = \frac{340}{670} = 0.5075 \simeq 0.51$

and $y = \frac{340}{2-0.51} = 228\ N/mm^2$

The value of 228 N/mm^2 for the maximum stress in reversed plane bending compares favourably to the value obtained by Gohn et al.[1] (240 N/mm^2 for a value of R equal to 0.4) This parameter can also be estimated by extrapolating the Goodman diagram as seen in Fig. 4, which gives a value of 220 N/mm^2.

The tensile fracture shown in Fig. 2 is a classical example of ductilefibrous fracture (often referred to as ductile fracture, dimple rupture or rupture). This type of fracture is simply large plastic deformation preceding separation. The separation is generally initiated at small particles (often not visible on fractographs) where cavities are formed. The cavities grow by plastic deformation under the increasing stress until the metal surrounding them flows apart. This mechanism is shown more clearly in Fig. 2(b) where the cavities are easily observed. These cavities may have been initiated at very small Cu_2O particles.

The fractographs in Fig. 3 show a PB102 strip specimen that had failed in fatigue. The crack propagation direction is from right to left in the photomicrographs.

The fatigue fracture mechanism may be divided into stages of crack nucleation, growth and fast propagation. Nucleation occurs generally at the surface by plastic deformation and growth takes place by repeated opening and closing of the crack, which gives rise to striations on the fracture surface. Some evidence of these striations is indicated by the circle drawn on Fig. 3(b). An 'overload' situation is subsequently reached and the propagation rate increases, which may give rise to crack branching, also present in Fig. 3b (bottom left) and alter the appearance of the fracture surface to transcrystalline or inter-crystalline; that is, cracking across the grains or along the grain boundaries. This fracture mode transition does not appear to have occurred in this case; indeed it is unlikely to occur in such a relatively ductile material.

After considering these stages of fatigue failure, the question arises as to the points in time, i.e. the number of cycles, at which crack nucleation, growth and fast propagation occur. In other words, is crack nucleation followed immediately by fast propagation or do nucleation and slow growth precede fast propagation? This aspect of fatigue failure in spring materials has yet to be elucidated.

6. CONCLUSIONS

1. The data obtained in fatigue testing, bending one-side-of-zero, is compatible with fatigue data obtained by testing in reversed plane bending; this finding enhances the validity of our data.

2. Tensile failure in the PB102 strip examined occurred by ductilefibrous fracture.

3. The topography of the fatigue fracture of PB102 strip was typical of a metal of this structural type.

7. FUTURE WORK

An attempt should be made to examine the nucleation and propagation of fatigue cracks in detail. A monitoring method used in the Fracture Mechanics approach to crack growth may be necessary to promote a better understanding of the problem.

8. REFERENCES

1. GOHN G.R., GUERARD J.P. and FREYNIK H.S. "The Mechanical Properties of Wrought Phosphor-Bronze Alloys," A.S.T.M. Special Technical Publication No. 183, 1956.

2. GRAY S.D. "The Fatigue Properties of Beryllium-Copper Strip," S.R.A. Research Report Number 205, August 1972.

3. THORNLEY J.C., Ph.D. Thesis, University of Bradford, 1970.

TABLE I Tensile Data for BS 2870 PB102 0.28 mm Strip

UNTIMATE TENSILE STRENGTH N/mm^2	HARDNESS HV 10	PROOF STRESS % (N/mm^2)			% ELONGATION (50 mm) GL
		0.1	0.2	0.5	
670	220	500	620	650	2

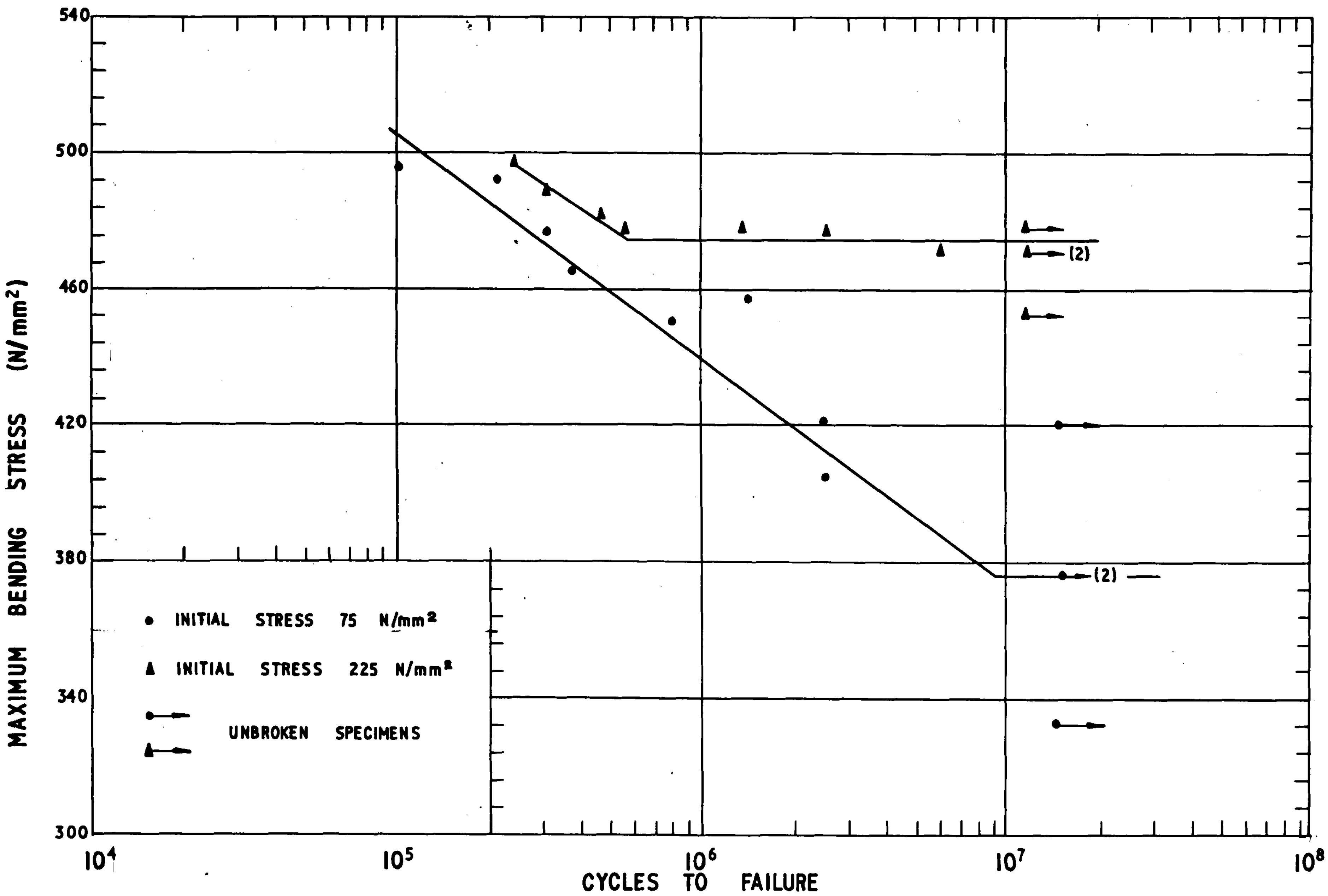

FIG. 1 S/N CURVES FOR 0·28 mm PB 102 SQUARE DRESSED EDGE STRIP

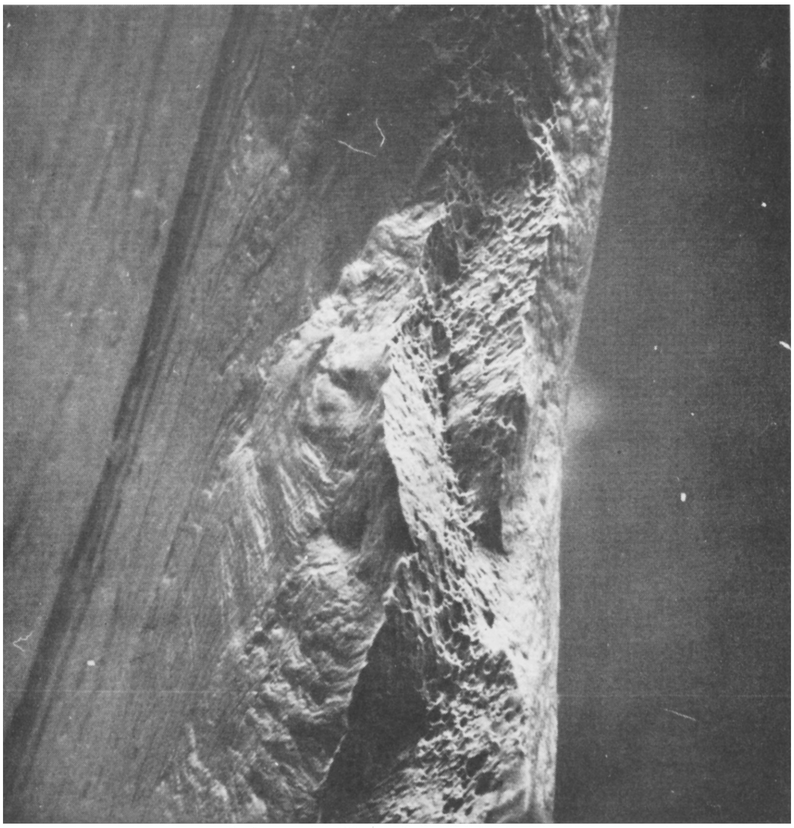

(a) magnification x 170

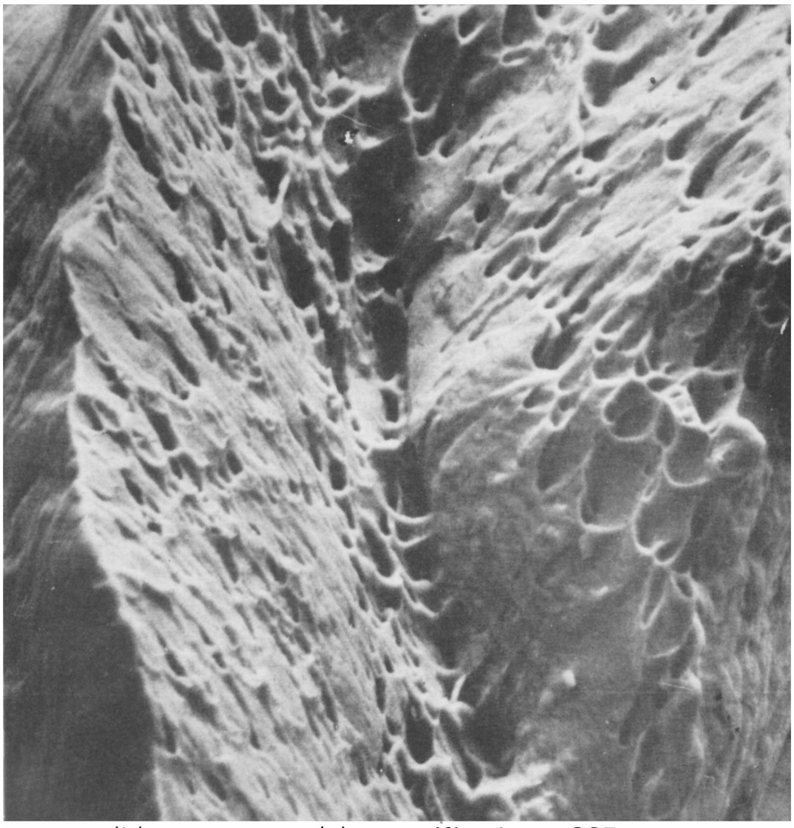

(b) same area as (a), magnification x 925

FIG. 2. Scanning Electron Micrographs Showing Ductilefibrous Fracture.

(a) magnification x 350

(b) different area than in (a), magnification x 750

FIG. 3. Scanning Electron Micrographs Showing Fatigue Fracture.

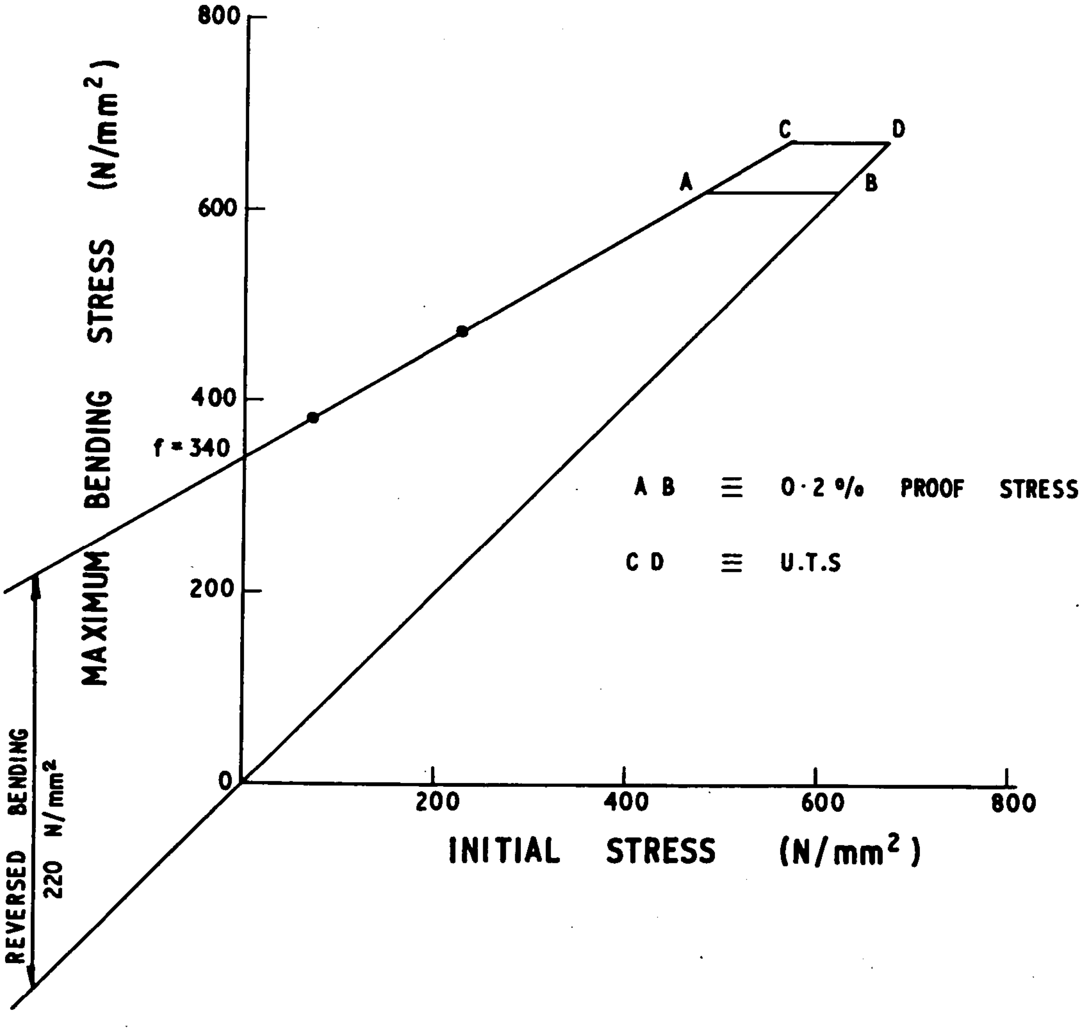

FIG. 4 MODIFIED GOODMAN DIAGRAM FOR 10^7 CYCLES, PB 102 0·28 mm SQUARE DRESSED EDGE STRIP.